THE ASTROPHYSICAL JOURNAL, 264:152–160, 1983 January 1

OBSERVATIONS OF THE EXTINCTION AND EXCITATION OF THE MOLECULAR HYDROGEN EMISSION IN ORION

S. BECKWITH,[1,2,3] NEAL J. EVANS II,[4] I. GATLEY,[5] G. GULL,[1] AND R. W. RUSSELL[1,6]
Received 1981 October 29; accepted 1982 June 24

ABSTRACT

We present the first observations of two quadrupole rotational transitions of molecular hydrogen, the $J = 7 \rightarrow 5$ and $9 \rightarrow 7$ transitions, along with several previously observed vibration-rotation H_2 lines in the Orion molecular cloud. The line ratios indicate a 2.1 μm extinction of approximately 2 mag. This extinction is intermediate between the earliest estimates of 4 mag and the more recent estimate of 1.2–2.0 mag. A comparison of the populations of three vibrational levels indicates a distribution of excitation temperatures between 1000 and 3000 K for the levels included; 1500 K best represents the temperature of the gas responsible for the $v = 1 \rightarrow 0$ line emission. These results imply the total luminosity of the molecular hydrogen emission is $200 \pm 80\ L_\odot$, and the mass of the emitting gas is of order $0.05\ M_\odot$. The uncertainties in the structure of the extinction and the geometry of the emission region may make it impossible to determine the luminosity and mass of the hot H_2 any more accurately. The mass and cooling time of the hot H_2 indicates at least $10\ M_\odot$ of material has been heated over the lifetime of the outflow.

Subject headings: interstellar: molecules — nebulae: Orion Nebula

I. INTRODUCTION

The molecular hydrogen emission from the core of the Orion molecular cloud has been the subject of exhaustive study since its discovery by Gautier *et al.* (1976) six years ago. The emission from Orion is the brightest and most luminous example of the known H_2 sources in the Galaxy, and it has therefore served as a prototype of such sources for comparison with theories for H_2 excitation. Although there is still some controversy about the details of the H_2 excitation, it is probably true that the emission results from high temperature regions occurring where outflowing matter in a wind or expanding shell mixes with the ambient cloud material (see, e.g., Shull and Beckwith 1982).

Several aspects of the H_2 line intensities are relevant to the study of the Orion star-forming region. For example, there has been a considerable amount of theoretical modeling of the conditions in the shock fronts in the mixed gas (Hollenbach 1982). There is currently an interest in the extent to which magnetic fields determine the structure of the shocked region and the H_2 line intensities. Recent models with magnetic fields predict a strong upper limit to the temperature of the shocked gas (Draine and Roberge 1982) that can in principle be verified through observations of the line intensities. Similarly, the total luminosity of the H_2 lines provides at least a lower limit to the energy dissipated by the outflowing gas as it encounters the cloud; when combined with estimates of the lifetime of the outflow, a lower limit can be derived for the total energy in the outflowing gas.

Both the excitation temperature and the foreground extinction to the region of H_2 excitation are derived from the relative intensities of different H_2 lines. The lines and methods used for these derivations are described by Gautier *et al.* (1976), Beckwith *et al.* (1978, hereafter BPNB), Beckwith, Persson, and Neugebauer (1979, hereafter BPN), Simon *et al.* (1979, hereafter SRJS), and Scoville *et al.* (1982, hereafter SHKR). The excitation temperature has so far been taken as 2000 K based on the ratio of one line from each of the $v = 2$ and $v = 1$ levels. If the molecules are excited in shock waves as suggested by the theoretical models, there should be some temperature structure which will show up as a variation in the excitation temperatures derived from different levels; there is already an indication of this effect from the observations of Beck, Lacy, and Geballe (1979). Measurements of the foreground extinction indicate an extinction of 1–4 mag at the wavelengths of the vibrational lines. The best presently available value is 1–2 mag (SHKR) based entirely on the reddening between two lines whose wavelengths differ by only 15% ($\Delta\lambda/\lambda$).

In this paper, we present observations of two previously unobserved H_2 lines, the $v = 0$–0 $S(5)$ and $S(7)$ lines, as well as accurate observations of several previously observed H_2 lines. Figure 1 is an energy level diagram for H_2 showing some of the transitions we observed. The line ratios give an independent estimate of

[1] Department of Astronomy, Cornell University.
[2] Visiting Astronomer, Kitt Peak National Observatory, which is operated by the Association of Universities for Research in Astronomy, Inc.
[3] Guest Investigator, United Kingdom Infrared Telescope Facility.
[4] Department of Astronomy and Electrical Engineering Research Laboratory, University of Texas at Austin.
[5] United Kingdom Infrared Telescope Facility.
[6] The Aerospace Corporation.

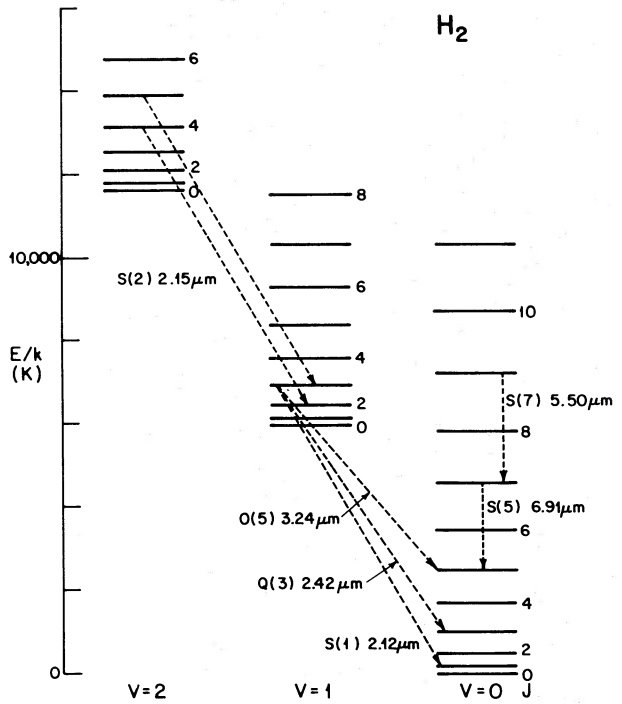

FIG. 1.—An energy level diagram showing the new $v = 0 \rightarrow 0$ transitions presented in this paper along with several previously detected lines for reference.

the foreground extinction and a more complete characterization of the excitation temperature than has previously been possible. In subsequent sections, the extinction, excitation, luminosity, and reddening law used to interpret the observations are discussed in light of the new data. In a final section, we discuss the mass of the H_2 and the structure of the emitting region.

II. OBSERVATIONS

The observations were made with a cooled grating spectrometer of the design described by Houck and Ward (1979). The instrument uses Cassegrain optics to collimate infrared radiation from a diaphragm in the focal plane of the telescope and direct it onto the grating in near-Littrow mode. The dispersed radiation is focused on a slit in the exit plane where a CaF_2 field lens concentrates it onto a solid-state detector. The incoming radiation is filtered with broad-band interference filters to isolate the grating order. The grating is a replica made by Bausch and Lomb, ruled at 150 grooves mm^{-1}, and blazed for 8 μm.

The different grating orders provide broad wavelength coverage as follows: fourth order, 1.8–2.3 μm; third order, 2.3–3.2 μm; second order, 3.2–5.0 μm; and first order, 5–9 μm. An InSb photovoltaic diode at 55 K covers the wavelengths shorter than 5.5 μm; a Si:Ga photoconducting diode at 4.2 K covers the longer wavelengths. The instrumental sensitivity is limited by radiation from the telescope and sky for wavelengths longward of about 3 μm.

We observed the 0–0 $S(7)$ and $S(5)$ rotational lines of H_2 in the direction of Pk 1 ($\alpha = 5^h32^m46^s.2$, $\delta = -5°24'02''$; all coordinates in this paper are epoch 1950) on the map of BPNB with NASA's Kuiper Airborne Observatory (KAO) at an altitude of 12.5 km during the last week of 1980 February. The spectral resolution was 0.011 μm for both wavelengths. The beam size was 26″ in diameter. The secondary mirror was oscillated at 30 Hz to provide a beam separation of 5′ for sky cancellation. Several measurements at each wavelength were made independently, and the measurements were subsequently averaged together. The total integration time per wavelength was about 3 minutes.

Observations of the standard stars α Ori and α UMa were used to calibrate the flux density scale. Puetter *et al.* (1977) give the flux density of α Ori between 4 and 8 μm, and we assumed the flux density of α UMa follows a Rayleigh-Jeans distribution with a flux density of 160 Jy at 7 μm. The sensitivities calculated from these stars agree within 15%, which is our estimate of the overall uncertainty in the flux density scale. It is possible, however, that absorption by narrow telluric features unresolved by our instrument affects the measurements of the narrow celestial lines. The spectra of the standard stars show that narrow telluric features account for no more than 15% absorption averaged over one spectral resolution element. The atmospheric absorption was also checked with the calculations of Traub and Stier (1976). The calculations imply that near the 0–0 $S(7)$ line, telluric absorption lines probably account for no more than 5% attenuation, and near the 0–0 $S(5)$ line, attenuation due to atmospheric lines is probably no greater than 20%. Visual guiding on θ^1 Ori C with an offset guider limited the absolute pointing uncertainty to about 5″. The standard stars were visible for direct guiding, and the peak-to-peak guiding uncertainty is 4″.

Spectra of krypton from a low-pressure lamp provided in-flight wavelength calibration. Spectra were taken several times in flight, before and after the observations of Orion and α Orionis. Seven krypton lines occur between 2 and 2.5 μm; when observed in third order, they provide coverage of most of the grating angles used at the long wavelengths. A comparison of the calibration curves at different times during the flight series indicates the uncertainty in the wavelength scale is of order one-half of the spectral resolution for the wavelength of the 0–0 $S(5)$ line. The wavelength of the 0–0 $S(7)$ line lies outside the range of grating angles covered by the calibration lamp. The calibration for this line was established by fitting the wavelengths of telluric water vapor lines which appear in the spectra of the standard stars.

The 2–1 $S(1)$, $S(2)$, $S(3)$, and 1–0 $S(0)$, $S(1)$, and $S(2)$ lines were observed toward the position of Pk 1 in 1979 December at the Cassegrain focus of the 2.1 m telescope at Kitt Peak National Observatory[7] (KPNO). The beam size was 10″ and the beam separation was 1′. The spectral resolution was of order 0.0025 μm for these observations. Measurements of argon lines from a fluorescent lamp

[7] Kitt Peak National Observatory is operated by the National Science Foundation.

established the wavelength calibration scale as described above, and the resulting wavelength scale is accurate to approximately one-quarter of a spectral resolution element. Observations of standard stars established the flux density scale. Eight different stars were measured several times during four nights. The sensitivities calculated from these observations were within 10% of the mean sensitivity at each wavelength for all stars. Interference by narrow telluric lines is potentially a problem for the 1–0 $S(2)$ and 2–1 $S(3)$ lines; we have not corrected for this affect.

The 1–0 $S(1)$, $S(2)$, $Q(3)$, $Q(4)$, $O(5)$, $O(6)$, and $O(7)$ lines were observed toward Pk 1 with the United Kingdom Infrared Telescope (UKIRT) at Mauna Kea, Hawaii, in 1980 October. The beam size was 4″ and the beam separation was 15″ in right ascension. The observing procedures were similar to those used at KPNO. Guiding uncertainties were about 2″ (peak-to-peak) for the UKIRT measurements. The guiding and calibration uncertainties dominated the system noise and account for much of the uncertainty in the results. We note that the beam separation used for these observations was not adequate to eliminate flux in the reference positions. Almost all the flux observed was produced by Pk 1 on the 5″ resolution map of BPNB, however, and the results should not be strongly affected by the small separation. Calibration of the flux density scale was made with only one standard star. We expect the flux density scale is probably accurate only to 20%, but the line ratios are accurate to 10%. Interference by narrow telluric lines is a potential problem for the 1–0 $O(5)$, $Q(3)$, and $Q(4)$ lines (cf. SHKR).

III. RESULTS

The observations of the purely rotational lines, the 0–0 $S(7)$ and $S(5)$ lines, are shown in Figure 2, and the observations of the 2–1 $S(3)$ and $S(2)$ lines are shown in Figure 3; the results of the observations are summarized in Table 1. The wavelengths in Table 1 were calculated using the constants of Fink, Wiggins, and Rank (1965). The intensities in Table 1 were calculated by fitting the instrumental profile function to the data; the fits are the solid lines in the figures. Three parameters were varied to obtain these fits: the amplitude and central wavelength of the profile function and the level of the continuum flux outside the line. The variation in amplitude which increased the χ^2 by one is the statistical uncertainty assigned to the flux density. Calibration uncertainties dominate the statistical uncertainties for all of the lines observed from the ground. The central wavelengths found by the fit agreed well with the calculated wavelengths.

Also given in Table 1 are the telescope and the diameter of the beam appropriate to each observation. The use of different beam diameters on the different telescopes makes direct comparison of the intensities impossible. Consequently, only ratios of line intensities will be used in the subsequent analysis. The 1–0 $S(1)$ line is used as a reference for the intensity ratios; its intensity is denoted I_1. The ratios of the line intensities (I) to the intensity of the 1–0 $S(1)$ line (I_1), observed with the same beam, are also given in Table 1. For the KAO observations, I_1 was estimated from the 30″ resolution map of Gautier (1978) to be 3.5×10^{-3} ergs s^{-1} cm^{-2} sr^{-1}.

As discussed in § IV, the ratio of the 1–0 $Q(3)$ and $S(1)$ lines is important for determinations of the extinction to the emitting region. Note that the UKIRT data indicate a value of 1.0 ± 0.1 for this ratio, while the KPNO data indicate 0.90 ± 0.09. For further analysis, we assume a value of 0.90 ± 0.09 for this ratio, which agrees with the results of SHKR to within the uncertainties. The small beam separation used for the UKIRT

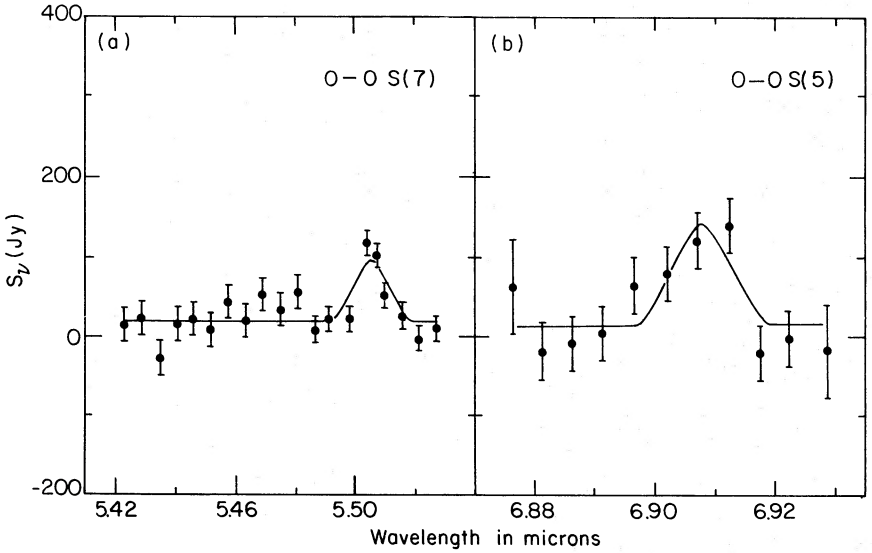

FIG. 2.—Measurements of the $v = 0 \rightarrow 0$ lines. The solid lines are least squares fits of the instrumental profile function to the data points as described in the text. The spectral resolution was approximately 0.011 μm for both lines.

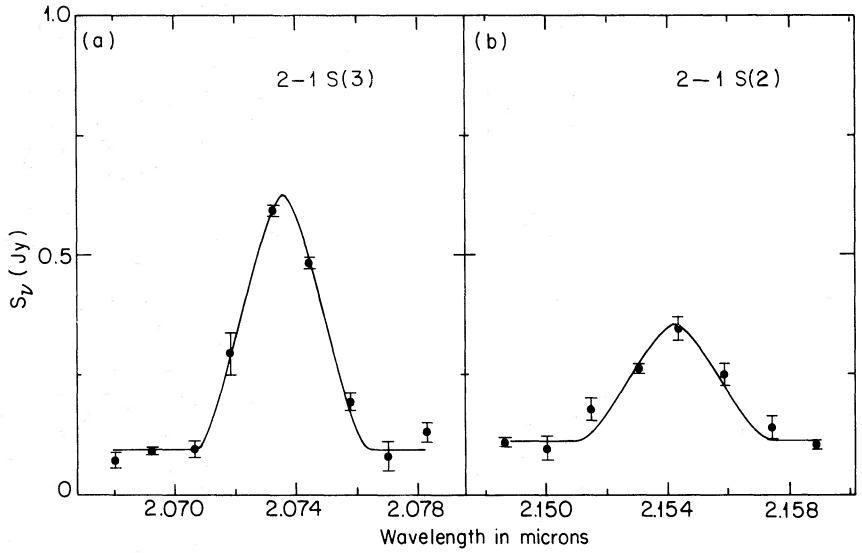

FIG. 3.—Measurements of the 2–1 $S(2)$ and $S(3)$ lines with the best fit instrumental profile functions

observations probably makes the ratio even less accurate than indicated by the formal uncertainty.

IV. THE EXTINCTION TO THE EMISSION REGION

Because all the H_2 emission lines are optically thin (Gautier *et al.* 1976; BPNB), the intensity of a line at wavelength λ may be written as follows:

$$I = \frac{Ahv}{4\pi} N(v_J) 10^{-A_\lambda/2.5} \text{ (ergs s}^{-1}\text{ cm}^{-2}\text{ sr}^{-1}\text{)}, \quad (1)$$

where A is the spontaneous decay rate in s^{-1}, h is Planck's constant, ν is the transition frequency in Hz, $N(v_J)$ is the column density of H_2 in cm^{-2} in the upper level (v_J) of the transition, and A_λ is the extinction at wavelength λ.

If the energy levels are in thermal equilibrium at a temperature T, then

$$N(v_J) = N \frac{g(v_J)}{Z} e^{-E(v_J)/kT}, \quad (2)$$

where N is the total column density, $g(v_J)$ is the statistical weight of level v_J, Z is the partition function, and $E(v_J)$ is the energy of level v_J. In the case of thermal equilibrium, the ratio of intensities for two lines is

$$\frac{I}{I_1} = \frac{Avg}{A_1 \nu_1 g_1} e^{-(E-E_1)/kT} 10^{-(A_\lambda - A_{\lambda_1})/2.5}, \quad (3)$$

where the quantum numbers have been suppressed for clarity. Assuming a temperature, the observed ratio and

TABLE 1

MOLECULAR HYDROGEN LINE INTENSITIES FROM ORION

Transition	λ (μm)	Telescope	Beam size	I (ergs^{-1} cm^{-2} sr^{-1})	I/I_1
0–0 $S(5)$	6.910	KAO	26″	$(9 \pm 3) \times 10^{-3}$	2.6 ± 0.9
0–0 $S(7)$	5.501	KAO	26″	$(7.5 \pm 1.5) \times 10^{-3}$	2.1 ± 0.4
1–0 $O(7)$	3.807	UKIRT	4″	2.0×10^{-3}	0.20 (10%)
1–0 $O(6)$	3.501	UKIRT	4″	1.2×10^{-3}	0.12 (10%)
1–0 $O(5)$	3.235	UKIRT	4″	5.8×10^{-3}	0.58 (10%)
1–0 $Q(4)$	2.438	UKIRT	4″	2.4×10^{-3}	0.24 (10%)
1–0 $Q(3)$	2.424	UKIRT	4″	1.0×10^{-2}	1.00 (10%)
1–0 $S(1)$	2.122	UKIRT	4″	1.0×10^{-2}	1.00
1–0 $S(2)$	2.034	UKIRT	4″	2.7×10^{-3}	0.27 (10%)
2–1 $S(1)$	2.248	KPNO	10″	5.7×10^{-4}	0.083 (10%)
2–1 $S(2)$	2.154	KPNO	10″	2.4×10^{-4}	0.035 (15%)
2–1 $S(3)$	2.074	KPNO	10″	5.9×10^{-4}	0.086 (10%)
1–0 $Q(3)$	2.424	KPNO	10″	6.2×10^{-3}	0.90 (10%)
1–0 $S(0)$	2.223	KPNO	10″	1.7×10^{-3}	0.25 (5%)
1–0 $S(1)$	2.122	KPNO	10″	6.9×10^{-3}	1.00
1–0 $S(2)$	2.034	KPNO	10″	2.1×10^{-3}	0.30 (10%)

equation (3) can be used to calculate the reddening $(A_\lambda - A_{\lambda_1})$ relative to the reference line at λ_1. By assuming an extinction law, the total extinction at λ_1 (A_{λ_1}) may also be inferred. As noted above, the 1–0 $S(1)$ line at 2.122 μm has been chosen as the reference line for all work on this region.

Because the excitation temperature may be uncertain, it is convenient to choose two lines arising in the same upper state. The extinction determinations by BPN, SRJS, and SHKR compare the 1–0 $S(1)$ and $Q(3)$ lines at 2.122 and 2.424 μm to obtain an estimate of $A_{2.424}-A_{2.122}$. Using an assumed extinction curve (in this case, van de Hulst's curve #15 described by Johnson [1968], which we will refer to as vdH), $A_{2.122}$ has been estimated. The most reliable value obtained from this technique is 1.2–2 mag given by SHKR, it can be shown that the values of 4 mag given by BPN and SRJS resulted from observational errors (see Geballe, Russell, and Nadeau 1982). There are some discrepant determinations which should be addressed. First, Knacke and Young (1981) estimate a 2.122 μm extinction of 4 mag based on their measurements of pure rotational lines between 3 and 4 μm. Second, SJRS noted that the reddening derived for the ratio of the 1–0 O branch lines at 3.5 and 3.8 μm relative to the 1–0 S and Q branch lines is inconsistent with the assumed reddening curve (vdH). As noted below, our results for the O branch lines essentially confirm this result.

Even if $A_{2.424}-A_{2.122}$ could be determined exactly, there would still be a large uncertainty in $A_{2.122}$ owing to the uncertainty in the reddening law used to determine the ratio $A_{2.122}/(A_{2.424}-A_{2.122})$. Previously, the vdH curve (approximately $\lambda^{-1.9}$ in the 2 μm region) was used to calculate this ratio, but the vdH curve was measured through relatively diffuse interstellar dust, and several different laws have been established for different environments. Sneden *et al.* (1978) and Elias (1978) found that λ^{-1} applies to many regions, whereas Jones and Hyland (1980) favor a $\lambda^{-2.5}$ law in their studies. If $A_\lambda \sim \lambda^{-\beta}$ with β between 1 and 2.5, when the ratio $A_{2.122}/(A_{2.424}-A_{2.122})$ is between -8.0 and -3.5, so there is at least a factor of 2 uncertainty in $A_{2.122}$.

The uncertainty in the ratio is substantially reduced if one of the two lines is at a long wavelength, because in this case the reddening is almost the same as the total extinction at the short wavelength. The 0–0 $S(7)$ line at 5.5 μm is useful for just this purpose. This line arises in a level whose energy (E/k) is only 243 K above the $v_J = 1_3$ level $(E/k = 6950$ K); the temperature dependence of the line intensity ratio 0–0 $S(7)$/1–0 $S(1)$ is therefore very weak, assuming both levels are thermalized. The unreddened theoretical ratio varies by only $\pm 6\%$ for temperatures between 1000 and 2000 K, and we have listed the theoretical ratio for an excitation temperature of 1500 K in Table 2 in anticipation of the results in § V. The extinction is estimated from the reddening between 5.507 and 2.122 μm as described above. We calculated the total extinction at 2.122 μm using both the vdH reddening law, and $A_\lambda \sim \lambda^{-\beta}$ with $\beta = 1$ and 2.5, and we find $A_{2.122} = 1.7$ to 2.5 mag for the different reddening laws. $A_{2.122}$ is much more strongly constrained by the use of the 0–0 $S(7)$ line than by the use of the 1–0 $Q(3)$ line.

The 2.122 μm extinction derived from this method is in good agreement with the results of SHKR considering the uncertainties in both methods. We obtain a range of 1.7–2.5 mag for $A_{2.122}$, where the range mainly reflects the different forms of the reddening law used to calculate total extinction. There are several potentially large uncertainties in this estimate discussed below, and there are also large uncertainties in the estimate based on 2 μm lines only. For the purpose of this discussion, however, it is very encouraging that substantially independent measurements of the extinction using different beam sizes, different wavelengths, and different reddening laws give reasonably consistent results. The uncertainties are sufficiently great that the quoted range is probably an underestimate of the real uncertainty in the extinction, but the results at least indicate an extinction at 2.122 μm of approximately 2 mag in the direction of Pk 1.

Observations were also made of the 1–0 $Q(3)$ and $O(5)$ lines in the direction of Pk 1 relative to the 1–0 $S(1)$ line. The reddening implied by these observations is used to calculate a 2.122 μm extinction for comparison with the above results. The 1–0 $Q(3)/S(1)$ ratio observed here agrees with that observed by SHKR to within the uncertainties but is undoubtedly less accurate owing to the relatively low spectral resolution of this experiment and the telluric interference at the wavelength of the $Q(3)$ line. The observed $O(5)/S(1)$ ratio is much smaller than expected from any of the reddening curves considered here. The atmospheric transmission is extremely poor near the wavelength of the $O(5)$ line, and it is quite likely that the observed line ratio is affected by poor correction for atmospheric attenuation in this case. In § VI, it will be shown that the 1–0 $O(6)$ and $O(7)$ lines are also weaker than expected for a standard reddening law, but in this case the observations are probably accurate.

We have made several assumptions which may be

TABLE 2

EXTINCTION RESULTS

Transition	λ (μm)	$(I/I_1)_{obs}$	$(I/I_1)_{unred}$	$A_\lambda - A_{2.122}$	λ^{-1} $A_{2.122}$	vdH $A_{2.122}$	$\lambda^{-2.5}$ $A_{2.122}$
0–0 $S(7)$	5.501	2.1 ± 0.4	0.507	-1.53 ± 0.19	2.49 ± 0.31	2.08 ± 0.26	1.69 ± 0.21
1–0 $Q(3)$	2.424	0.95 ± 0.10	0.701	-0.33 ± 0.11	2.65 ± 0.88	1.68 ± 0.56	1.17 ± 0.39
1–0 $O(5)$	3.235	0.58 ± 0.06	0.395	-0.42 ± 0.11	1.22 ± 0.32	0.87 ± 0.23	0.64 ± 0.17

incorrect depending on the geometry and density of the H_2 emission region. Specifically, we have assumed the intensity of the 1–0 $S(1)$ line in a 26″ beam can be reliably estimated from the map of Gautier, that the 1–0 $S(1)$ and 0–0 $S(7)$ lines arise from the same gas, that the spontaneous emission rates for the 1–0 $S(1)$ and 0–0 $S(7)$ lines are well known, and that the levels are thermalized or very closely thermalized. These assumptions are discussed below.

We expect the uncertainty in the $S(1)$ flux is less than the 20% statistical uncertainty in the 0–0 $S(7)$ flux. Both Gautier's map and the map of BPNB made with 13″ resolution show contours which fall off smoothly from the peak intensity in the direction of Pk 1. The peak intensities of both maps are consistent when beam dilution is accounted for. Thus although the H_2 emission appears clumpy at very high spatial resolution, it is relatively smooth at low resolution, and it should therefore be relatively easy to estimate the peak surface brightness in the 26″ beam.

Whether or not the long and short wavelength lines arise from the same gas depends largely on the (unknown) internal extinction of the emission region. Selection of lines with very similar upper state energies ensures that the lines arise from gas at very similar temperatures. If the emission region is extended along the line of sight with substantial internal extinction as suggested by Nadeau and Geballe (1979), Beck (1982), and Nadeau, Geballe, and Neugebauer (1982), then the long wavelength lines will originate deeper in the cloud on average than the short wavelength lines. This problem will plague *any* two lines used to estimate a foreground reddening, and although it has a smaller effect on two lines at nearby wavelengths, the effect is amplified when the extrapolation from reddening to total extinction is made. The effect can be estimated for the lines presented here with a model for the internal extinction. If we approximate the H_2 emission region as consisting of a spherical shell with 3 mag of extinction at 2.122 μm within the shell, then the observed ratio of the 0–0 $S(7)$/1–0 $S(1)$ lines implies a *foreground* extinction (extinction in front of the shell) of 1.7–2.2 for the vdH and λ^{-1} laws, respectively. While the actual structure of the region is probably much more complex than assumed for this example, this model can explain the asymmetry of the 2 μm line profile observed in the direction of Pk 1 (Nadeau, Geballe, and Neugebauer 1982), and should be representative of the magnitude to which internal extinction will affect the estimate of foreground extinction.

The spontaneous emission rates calculated by Turner, Kirby-Docken, and Dalgarno (1977) should be accurate to a few percent or better for the 0–0 $S(7)$ and 1–0 $S(1)$ lines (Dalgarno, personal communication). The uncertainties in the calculations depend primarily on uncertainties in the frequencies of the transitions, since the rates are proportional to the fifth power of the frequency. The measurements by Knacke and Young (1981) of the frequencies of the 0–0 $S(15)$ through 0–0 $S(8)$ lines in Orion show that the observed frequencies are within one part in 3000 of those predicted by theory.

Finally, the unreddened line intensity ratios could be different from those calculated here if the level populations are not in thermal equilibrium. In the next section, we argue that the level populations strongly support the assumption of thermal equilibrium, but some recent shock models for the production of H_2 emission in Orion suggest otherwise (Draine and Roberge 1982). Since the models depend strongly on poorly known collisional rates, magnetic field strengths, and densities, it is difficult to estimate the uncertainty in our assumption, but we note that the results may be affected if the levels are not thermalized.

V. TEMPERATURE AND LUMINOSITY

The line intensity ratios can be corrected for extinction, using either the $\lambda^{-\beta}$ or the vdH extinction law, together with the value of $A_{2.122}$ appropriate to that law. Defining $\mathcal{N}(v_J) \equiv N(v_J)/g(v_J)$, the column density per degenerate sublevel, and $\mathcal{E}(v_J) \equiv E(v_J)/k$, equation (2) implies that

$$\ln \frac{\mathcal{N}(v_J)}{\mathcal{N}(1_3)} = -\frac{1}{T}[\mathcal{E}(v_J) - \mathcal{E}(1_3)], \qquad (4)$$

if the levels are thermalized. The ratios $\mathcal{N}(v_J)/\mathcal{N}(1_3)$ are determined from the corrected line intensities via equation (1). We will assume in what follows that the temperatures derived from equation (4) are representative of the kinetic temperatures where the H_2 emission arises.

The results are plotted in Figure 4, along with the best-fitting straight lines to various restricted data sets. The data indicate a flattening of the slope, or increase in T, for lines arising from higher energy states. Such a trend is expected if there is a distribution of temperatures along the line of sight, because the lines requiring higher excitation energy will sample mainly the hotter gas. Evidence for temperature variations has already been presented by Beck, Lacy, and Geballe (1979), who found that a substantial column density of H_2 cooler than 2000 K must be present to account for the strength of the 0–0 $S(2)$ line.

In this situation, a variety of temperatures must be considered. The vibrational temperature $T_v(1, 2)$ characterizing the relative populations in the $v_J = 2_3$ and 1_3 levels is $T_v \approx 1900$ K, similar to that found by BPNB. The vibrational temperature $T_v(0, 1)$ characterizing the 1_3 and 0_4 levels is only 1100 K. The rotational temperature in the $v = 2$ states $T_R(v = 2) \approx 3000$ K. The rotational temperature in the $v = 0$ states, $T_R(v = 0)$, determined *only* by the two lines observed here, is 1500 K, justifying the assumption made in § IV. The rotational temperature in the $v = 1$ states, $T_R(v = 1)$, is also ~ 1500 K (the KPNO observations give 1600 K, and the UKIRT observations give 1200 K). The 1–0 O branch lines were not used in the determination of $T_R(v = 1)$ because the extinction corrections are very uncertain as discussed in the last section. A separate fit to these lines alone gave $T_R(v = 1) \approx 1600$ K. Separate fits were obtained for data

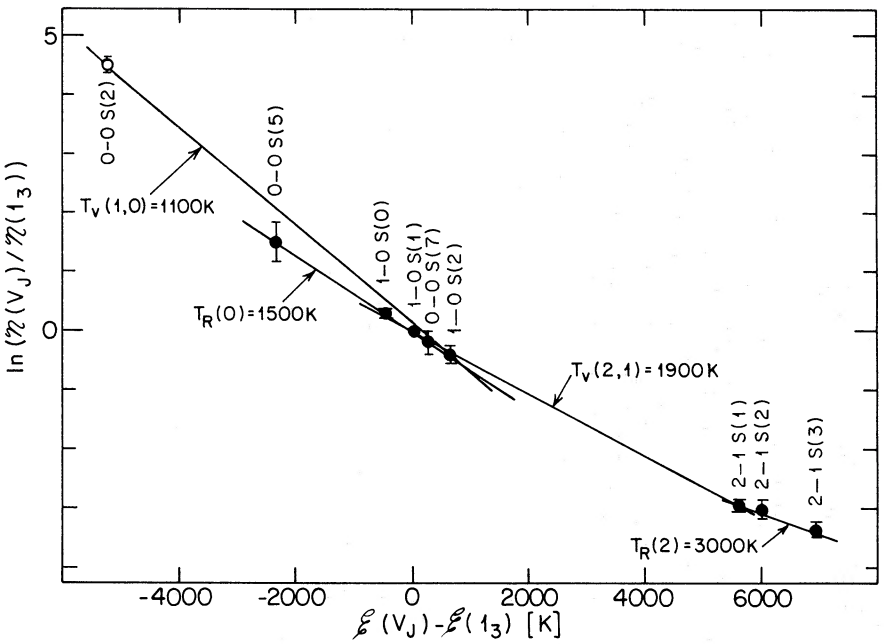

FIG. 4.—A plot of the column density per sublevel $N(v_J)$ of hydrogen molecules in the v_J level relative to $N(1_3)$ versus the energy (K) of the level above that of the 1_3 state $[\mathscr{E}(v_J) - \mathscr{E}(1_3)]$. The open circle is based on data by Beck, Lacy, and Geballe (1979). All data have been corrected for reddening by the λ^{-1} law. The 1–0 $S(0)$ and 1–0 $S(2)$ lines represent the KPNO data.

corrected with a λ^{-1} and a vdH law; the largest difference in the derived temperature was 140 K, which is not significant; hence, the results given above are averages of the results for the two extinction laws. The values shown in Figure 4 were calculated using a λ^{-1} extinction law. Additional extinction at the 12 μm 0–0 $S(2)$ line may result from silicates in the dust.

The total luminosity of all H_2 lines based on a thermal distribution at 1500 K and a foreground extinction of 1.7–2.5 mag is $200 \pm 80\ L_\odot$, where we have used 2.5 $L_\odot$ for the apparent luminosity of the 1–0 $S(1)$ line (BPNB). The primary uncertainty in this estimate is in the extinction. This is especially true because the 1–0 $S(1)$ line probably suffers considerable extinction within the region of the line formation, and variations in both foreground and internal extinction could hide regions of substantial emission. A map of the 0–0 $S(7)$ line could determine if this is the case. The ratio of total H_2 luminosity to 1–0 $S(1)$ luminosity depends only weakly on temperature. It is between 10 and 12 for temperatures between 1000 and 2000 K, and it rises to ~ 17 at 3000 K; below 1000 K, the H_2 luminosity drops so rapidly that even large amounts of cooler gas will not contribute substantially to the estimate.

The luminosity derived above is in good agreement with that of SHKR but is an order of magnitude lower than the estimates of BPN and SRJS. Most of the difference results from the lower extinction used here, but an additional factor of 2 comes from the incorrect calculation of total to 1–0 $S(1)$ line luminosity by the latter authors.

VI. THE REDDENING LAW

The total extinction at any one wavelength implied by the measurements in this paper depends on the form of the reddening law. The extinctions derived by BPN, SRJS, and SHKR depend even more critically on the shape of the extinction curve. It is useful to compare the two forms of the extinction law assumed in this paper with all of the data to check for consistency.

The extinction between 2 and 7 μm is particularly interesting because the reddening law is poorly determined for dense molecular clouds. In this spectral region, "clean" silicates are nearly transparent, whereas observations of stars and protostars embedded in clouds imply significant opacity, normally attributed to impurities (Jones and Merrill 1976). It is difficult to determine the reddening in clouds because the shape of the unreddened spectra of protostars is unknown, and rather severe radiative transfer effects make it very difficult to interpret the reddened spectra. Some of these difficulties can be avoided by comparing the intensity ratios of several narrow lines, as long as the unreddened ratios can be predicted accurately. The line ratios are often much easier to predict than continuum spectra, and the radiative transfer effects are not severe if the opacity is produced entirely by dust that is not heated significantly by the line radiation.

To compare the extinction laws, we use the following method. The unreddened intensity of each line is calculated relative to the 1–0 $S(1)$ line. The difference between the observed relative line intensities and the

unreddened intensities is assumed to be the result of the reddening between the wavelength of that line and 2.122 μm. This reddening, denoted $A_\lambda - A_{2.122}$, is plotted versus the line wavelength λ, and the distribution of $A_\lambda - A_{2.122}$ is compared to that implied by the two reddening laws in Figure 5.

The unreddened intensity ratios for the different lines were calculated assuming the levels were thermalized at the temperatures derived in § V for the separate levels (essentially 1500 K). The ratios of several of the lines are relatively insensitive to the choice of temperature, in particular 1–0 $Q(3)$, $O(5)$ and 0–0 $S(7)$ lines. The 1–0 $S(2)$, $Q(4)$, and $O(6)$ lines originate in the same upper level, so their relative ratios are independent of the excitation temperature. The intensity ratios of the other lines used for Figure 5 depend somewhat more strongly on temperature. For each of the lines in the figure, we have indicated the reddening that would be implied by a different choice for the excitation temperature, both for 1000 K and 3000 K, using different symbols to denote the different temperatures. When only one symbol is present, the change in reddening introduced by assuming a different excitation temperature is negligible.

Based on Figure 5, the two extinction laws are equally good at representing the data. It should be noted that an extrapolation from the 1–0 $Q(3)/S(1)$ reddening alone depends very strongly on the assumed law. It is also interesting to note that both extinction laws appear to underestimate the extinction in the 3.2–3.7 μm range as found by SRJS. Since the 3.5–3.7 μm region typically does not show strong absorption in the spectra of objects embedded deeply in clouds (Soifer *et al.* 1979), it would be interesting to establish this result in another cloud using the H_2 line ratios. Study of other lines arising from states with similar energies, but occurring at different wavelengths, together with models for the temperature structure of the emission region could lead to much improved knowledge of the reddening law in the mid-infrared.

VII. THE STRUCTURE OF THE EMITTING REGION

The mass of the hot H_2, while relatively small, is indicative of a considerable mass in cooler associated gas. For assumed gas temperatures between 1500 and 2000 K and $A_{2.122}$ of 2 mag, the mass of gas now emitting molecular hydrogen lines is 0.03–0.07 $M_\odot$. Because the gas cools to less than 1000 K in a time of order three years (Kwan 1977), this mass must be continuously replenished by newly swept-up shocked gas as the region evolves. If the lifetime of the region is of order 1000 years (see, e.g., Beckwith 1981), 10 $M_\odot$ or more has been processed through hot H_2 over the lifetime of the expanding region. This is the same order as the mass derived for the CO plateau feature. We expect this cooler gas has velocities comparable to the H_2 velocities, which is the case for the CO plateau feature.

If the plateau feature originates primarily in swept-up gas, the outflow from the infrared cluster may be at much

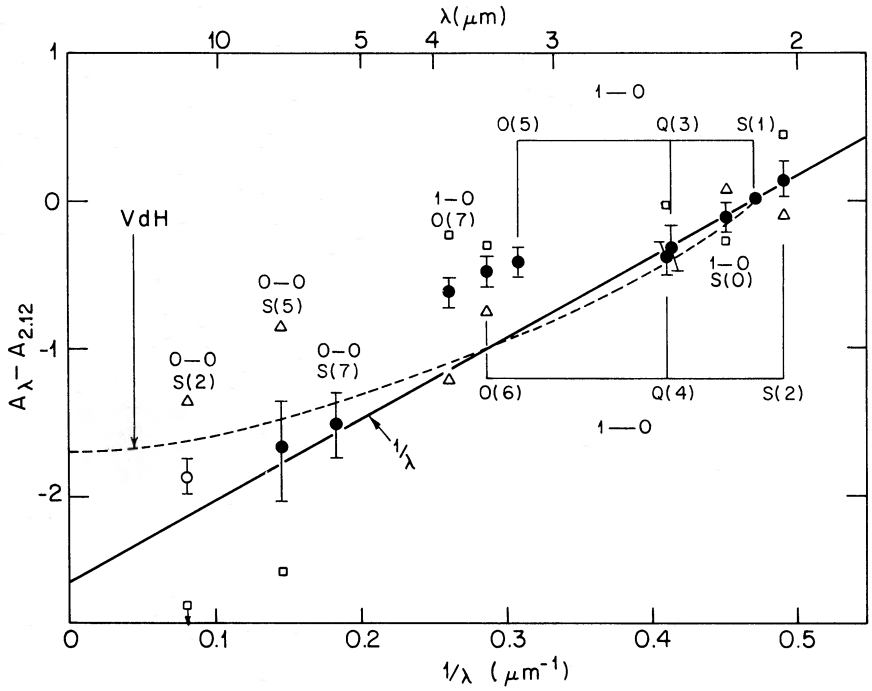

FIG. 5.—The reddening ($A_\lambda - A_{2.122}$) deduced from line ratios is plotted versus wavelength. The open circle is based on data by Beck, Lacy, and Geballe (1979). The horizontal scale is linear with inverse wavelength. The unreddened line ratios were calculated for assumed temperatures found in § V (*solid circles*), 1000 K (*open triangles*), and 3000 K (*open squares*). When open triangles or squares do not appear, the change introduced by assuming a different temperature is smaller than the measurement uncertainties. Two sets of lines originate from a common upper level as noted in the figure. The sense of the vertical axis is that it represents less reddening relative to 2.122 μm; *less* reddening indicates *extra* extinction above the amount predicted by the λ^{-1} or vdH curve.

higher velocities than the highest observed plateau feature velocities. If the outflow results from a wind from one of the stars in the infrared cluster, it may be possible to identify the candidate stars by looking for outflow at velocities of several hundred kilometers per second or more in material very close to the objects. We note that Scoville (1981) detected Bγ emission from the BN object out to ± 200 km s^{-1}, and it is possible that sensitive spectra of some of the other infrared stars will show high-velocity lines as well. We believe a link between the gas velocities very close to a star and those which drive the gas in the outer portions of the expanding region is necessary to identify the source of the outflow, and that any of the objects in the infrared cluster might still be regarded as candidates for the source.

VIII. SUMMARY

We have observed the purely rotational 0–0 $S(7)$ and $S(5)$ lines of H_2 in the Orion molecular cloud along with several vibration-rotation H_2 lines. The observational results may be summarized as follows:

1) A comparison of the 0–0 $S(7)$ and $S(1)$ lines of H_2 at 5.5 and 2.12 μm, respectively, implies an average extinction to the H_2 emission in Orion of about 2 mag at 2.12 μm.

2) A distribution of temperatures characterizes the level populations, which appear to be in local thermodynamic equilibrium. The temperatures range from 1000 K for the lowest purely rotational levels to 3000 K for the highest vibrational levels. This range of temperatures is consistent with the interpretation that the H_2 is excited thermally in shock-heated gas which cools after passage of the shock front.

3) The total luminosity of the hot molecular hydrogen is $200 \pm 80\ L_\odot$ with a large uncertainty caused mainly by the uncertainty in the overall extinction. There may be additional luminosity not presently seen at 2.12 μm if substantial extinction occurs within the emission region itself.

We are grateful to the staffs of the Kuiper Airborne Observatory, Kitt Peak National Observatory, and the United Kingdom Infrared Telescope for the excellent support they gave to this project. Without their assistance, these observations would have been impossible. We thank L. DeNoyer for assistance with the observations at Kitt Peak under difficult circumstances, and J. Houck for providing the Dewar and basic spectrometer design and for loan of the offset guider on the KAO. We profited from discussion with S. Beck, A. Dalgarno, B. Draine, J. Storey, and C. H. Townes, and comments from the referee. We are grateful to S. Corbin and B. Davidson for assisting with the preparation of the manuscript. This research was supported by NASA grant NSG 2412, and the instrument was built with funds from the Research Corporation. Partial support was obtained from NSF grant AST 79-20966.

REFERENCES

Beck, S. C., 1982, Ph.D. thesis, University of California at Berkeley.
Beck, S. C., Lacy, J. H., and Geballe, T. R. 1979, *Ap. J. (Letters)*, **234**, L213.
Beckwith, S., 1981, in *IAU Symposium 96, Infrared Astronomy*, ed. D. P. Cruikshank and C. G. Wynn-Williams (Dordrecht: Reidel).
Beckwith, S., Persson, S. E., and Neugebauer, G. 1979, *Ap. J.*, **227**, 436 (BPN).
Beckwith, S., Persson, S. E., Neugebauer, G., and Becklin, E. E. 1978, *Ap. J.*, **223**, 464 (BPNB).
Draine, B. T., and Roberge, W. G. 1982, preprint.
Elias, J. H. 1978, *Ap. J.*, **223**, 859.
Fink, U., Wiggins, T. A., and Rank, D. H. 1965, *J. Molec. Spectrosc.*, **18**, 384.
Gautier, T. N., III. 1978, Ph.D. thesis, University of Arizona.
Gautier, T. N., III, Fink, U., Treffers, R. R., and Larson, H. P. 1976, *Ap. J. (Letters)*, **207**, L129.
Geballe, T. R., Russell, R. W., and Nadeau, D. 1982, *Ap. J. (Letters)*, **259**, L47.
Hollenbach, D. J. 1982, *Proc. NY Acad. Sci. (Draper Symp.)*, in press.
Houck, J. R., and Ward, D. 1979, *Pub. ASP*, **91**, 140.
Johnson, H. L., 1968, in *Stars and Stellar Systems*, Vol. **7**, *Nebulae and Interstellar Matter*, ed. B. M. Middlehurst and L. H. Aller (Chicago: University of Chicago Press), p. 167.
Jones, T. W., and Hyland, A. R. 1980, *M.N.R.A.S.*, **192**, 359.
Jones, T. W., and Merrill, K. M. 1976, *Ap. J.*, **209**, 509.
Knacke, R. F., and Young, E. T. 1981, *Ap. J. (Letters)*, **249**, L65.
Kwan, J. 1977, *Ap. J.*, **216**, 713.
Nadeau, D., and Geballe, T. R. 1979, *Ap. J. (Letters)*, **230**, L169.
Nadeau, D., Geballe, T. R., and Neugebauer, G. 1982, *Ap. J.*, **253**, 154.
Puetter, R. C., Russell, R. W., Sellgren, K., and Soifer, B. T. 1977, *Pub. ASP*, **89**, 320.
Scoville, N. Z. 1981, in *IAU Symposium 96, Infrared Astronomy*, ed. D. P. Cruikshank and C. G. Wynn-Williams (Dordrecht: Reidel).
Scoville, N. Z., Hall, D. N. B., Kleinman, S. G., and Ridgeway, S. T. 1982, *Ap. J.*, **253**, 136 (SHKR).
Shull, J. M., and Beckwith, S. 1982, *Ann. Rev. Astr. Ap.*, **20**, in press.
Simon, M., Righini-Cohen, G., Joyce, R. R., and Simon, T. 1979, *Ap. J. (Letters)*, **230**, L175 (SRJS).
Sneden, C., Gehrz, R. D., Hackwell, J. A., York, D. G., and Snow, T. P. 1978, *Ap. J.*, **223**, 168.
Soifer, B. T., Puetter, R. C., Russell, R. W., Willner, S. P., Harvey, P. M., and Gillett, F. C. 1979, *Ap. J. (Letters)*, **232**, L53.
Traub, W. A., and Stier, M. T. 1976, *Appl. Optics*, **15**, 364.
Turner, J., Kirby-Docken, K., and Dalgarno, A. 1977, *Ap. J. Suppl.*, **35**, 281.

STEVEN BECKWITH: Astronomy Department, 230 Space Sciences Building, Cornell University, Ithaca, NY 14853-0352

NEAL J. EVANS, II: Astronomy Department, University of Texas, Austin, TX 78712

IAN GATLEY: United Kingdom Infrared Telescope, 900 Leilani Street, Hilo, HI 96720

GEORGE GULL: 201 Space Sciences Building, Center for Radiophysics and Space Research, Cornell University, Ithaca, NY 14853-0355

RAY W. RUSSELL: The Aerospace Corporation, A6/2617, Space Sciences Laboratory, IR Group, P.O. Box 92957, Los Angeles, CA 90009